Inorganic Chemistry

Article

pubs.acs.org/IC

Uranyl and Uranyl–3d Block Cation Complexes with 1,3-Adamantanedicarboxylate: Crystal Structures, Luminescence, and Magnetic Properties

Pierre Thuéry,*[,†] Eric Rivière,[‡] and Jack Harrowfield[§]

[†]CEA, IRAMIS, CNRS UMR 3685 NIMBE, LCMCE, Bât. 125, 91191 Gif-sur-Yvette, France

[‡]Université Paris-Sud 11, ICMMO, UMR 8182, Bât. 420, 91405 Orsay, France

[§]Université de Strasbourg, ISIS, 8 allée Gaspard Monge, 67083 Strasbourg, France

Supporting Information

ABSTRACT: The reaction of 1,3-adamantanedicarboxylic acid (LH_2) with uranyl nitrate under solvo-hydrothermal conditions, either alone or in the presence of additional metal cations (Co^{2+}, Ni^{2+}, or Cu^{2+}) gives a series of nine complexes displaying a wide range of architectures. While $[UO_2(L)(H_2O)]\cdot 1.25CH_3CN$ (**1**) and $[UO_2(L)(DMF)]$ (**2**) are one-dimensional (1D) species analogous to that previously known, $[H_2NMe_2]_2[(UO_2)_2(L)_3]\cdot 1.5H_2O$ (**3**), which includes dimethylammonium counterions generated in situ, is a three-dimensional (3D) framework, and $[UO_2(L)(NMP)]$ (**4**) (NMP = *N*-methyl-2-pyrrolidone) is a braid-shaped 1D polymer. When 3d block metal ions are present and bound to 2,2′-bipyridine (bipy) coligands, their role is reduced to that of decorating species attached to uranyl-containing 1D polymers, as in $[UO_2M(L)_2(bipy)_2]\cdot 0.5H_2O$ with M = Co (**5**) or Ni (**6**), and $[(UO_2)_2Cu_2(L)_3(NO_3)_2(bipy)_2]\cdot 0.5H_2O$ (**9**), or of counterions, as in $[Ni(bipy)_3][(UO_2)_4(O)_2(L)_3]\cdot 3H_2O$ (**7**), in which a two-dimensional (2D) assembly is built from tetranuclear uranyl-containing building units. In contrast, the heterometallic 3D framework $[UO_2Cu(L)_2]$ (**8**) can be isolated in the absence of bipy. The emission spectra measured in the solid state display the usual uranyl vibronic fine structure, with various degrees of resolution and quenching, except for that of complex **7**, which shows emission from the nickel(II) centers. The magnetic properties of complexes **5**, **6**, **8**, and **9** were investigated, showing, in particular, the presence of zero-field splitting effects in **6** and weak antiferromagnetic interactions in **9**.

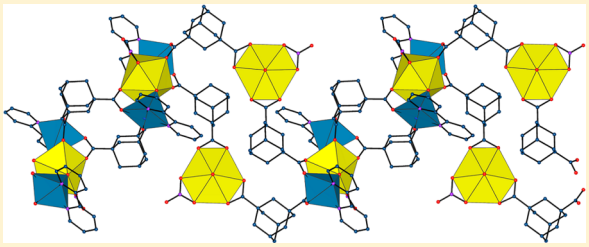

INTRODUCTION

Polycarboxylic acids based on the cyclohexane ring platform have lately been shown to be extremely versatile ligands for the synthesis of uranyl–organic discrete polynuclear species as well as coordination polymers, networks, or frameworks.[1] In contrast with the benzenic polycarboxylic acids that have been much investigated in uranyl chemistry,[2] the uranyl complexes with these alicyclic analogues were until very recently limited to those with cyclohexane-1,3-dicarboxylic acid, which gives one- and two-dimensional (1D and 2D) assemblies,[3] and with all-*cis*-1,2,3,4,5,6-cyclohexanehexacarboxylic acid, which is found in 2D uranyl–lanthanide(III) heterometallic species,[4] with some other examples including derivatives such as a monoester of Kemp's triacid, which gives an octanuclear uranyl cage,[5] and bicyclo[2.2.2]oct-7-ene-2,3,5,6-tetracarboxylic acid, which affords a 2D assembly.[6] In its reactions with uranyl ions under solvo-hydrothermal conditions, Kemp's triacid itself (*cis*,*cis*-1,3,5-trimethylcyclohexane-1,3,5-tricarboxylic acid) was latterly shown to be very sensitive to the choice of the organic cosolvent and the presence of additional cations, thus giving various species ranging from quite unremarkable 1D or 2D coordination polymers to unusual discrete or 1D species, metallacyclic, cage-like, or nanotubular.[7] While the axial position of the acid groups in this ligand is conducive to the formation of polynuclear, closed species, a nanotubular assembly was also obtained with all-equatorial 1,3,5-cyclohexanetricarboxylic acid, beside various 2D and three-dimensional (3D) architectures.[8] All these results prompted us to undertake the investigation of other ligands in this family, and the present work involves the geometrically constrained 1,3-adamantanedicarboxylic acid (LH_2), in which the two acid groups are necessarily equatorial. The synthesis and crystal structure of a uranyl complex with L^{2-} have previously been reported, this compound crystallizing as a 1D coordination polymer in which the carboxylate groups are either chelating or bridging bidentate.[9] This compound having been synthesized under purely hydrothermal conditions, it appeared worthwhile to introduce variations in the experimental setup so as to possibly generate complexes with different architectures and higher dimensionalities. We report herein the synthesis and crystal structure of nine uranyl complexes with L^{2-} obtained under solvo-hydrothermal conditions with various organic cosolvents, as well as, in most

Received: December 16, 2014
Published: February 24, 2015

DOI: 10.1021/ic503004j
Inorg. Chem. 2015, 54, 2838–2850

Table 1. Crystal Data and Structure Refinement Details

	1	2	3	4	5	6	7	8	9
chemical formula	$C_{14.5}H_{19.75}N_{1.25}O_7U$	$C_{15}H_{21}NO_7U$	$C_{40}H_{61}N_2O_{17.5}U_2$	$C_{17}H_{23}NO_7U$	$C_{44}H_{45}CoN_4O_{10.5}U$	$C_{44}H_{45}N_4NiO_{10.5}U$	$C_{66}H_{72}N_6NiO_{25}U_4$	$C_{24}H_{28}CuO_{10}U$	$C_{56}H_{59}Cu_2N_6O_{22.5}U_2$
M (g mol^{-1})	561.60	565.36	1325.97	591.39	1094.80	1094.58	2360.13	778.03	1779.23
cryst syst	monoclinic	triclinic	triclinic	monoclinic	monoclinic	monoclinic	triclinic	monoclinic	triclinic
space group	$P2_1/n$	$P\bar{1}$	$P1$	$C2/c$	$P2_1/c$	$P2_1/c$	$P\bar{1}$	$C2/c$	$P\bar{1}$
a (Å)	11.0329(3)	8.8534(8)	12.3331(7)	36.6031(16)	16.5351(8)	16.4567(9)	14.0975(5)	17.3216(11)	13.7842(7)
b (Å)	16.7685(5)	10.6080(11)	14.7388(8)	10.1698(4)	13.8250(5)	13.7860(5)	14.5802(3)	12.0844(8)	14.0430(5)
c (Å)	19.2896(3)	10.8364(9)	14.9946(8)	21.1750(8)	19.8753(7)	19.9056(11)	20.5052(7)	11.9978(6)	16.2606(7)
α (deg)	90	101.364(5)	111.546(2)	90	90	90	102.9388(17)	90	89.053(3)
β (deg)	94.4887(18)	112.692(4)	105.075(3)	110.279(4)	109.815(2)	109.587(3)	97.3018(15)	110.940(4)	82.825(2)
γ (deg)	90	105.953(5)	106.267(3)	90	90	90	114.3083(16)	90	80.931(3)
V (Å^3)	3557.73(15)	848.46(15)	2223.6(2)	7393.7(6)	4274.4(3)	4254.7(4)	3627.7(2)	2345.5(3)	3083.9(2)
Z	8	2	2	16	4	4	2	4	2
D_{calcd} (g cm^{-3})	2.097	2.213	1.980	2.125	1.701	1.709	2.161	2.203	1.916
μ (Mo Kα) (mm^{-1})	9.159	9.602	7.349	8.820	4.236	4.308	9.235	7.862	5.998
F(000)	2108	532	1278	4480	2160	2164	2212	1492	1718
reflns collcd	135 399	51 106	90 218	113 935	143 757	142 929	216 111	40 022	270 923
indep reflns	10 859	5181	16 727	9552	11 034	8072	18 707	2229	11 689
obsd reflns [$I > 2\sigma(I)$]	9398	4261	14 795	7081	7275	6415	15 588	1873	10 172
R_{int}	0.025	0.074	0.041	0.085	0.074	0.048	0.056	0.040	0.031
params refined	448	219	1117	471	550	550	946	165	802
R_1	0.025	0.032	0.044	0.035	0.037	0.035	0.028	0.031	0.050
wR_2	0.059	0.054	0.102	0.075	0.066	0.068	0.071	0.084	0.133
S	1.039	0.912	1.060	0.976	0.935	1.052	1.038	1.020	1.106
$\Delta\rho_{min}$ (e Å^{-3})	−1.89	−1.45	−0.85	−1.16	−1.17	−0.83	−1.66	−1.07	−1.89
$\Delta\rho_{max}$ (e Å^{-3})	2.00	1.43	1.35	1.51	1.10	0.84	1.80	2.46	5.45

DOI: 10.1021/ic503004j
Inorg. Chem. 2015, 54, 2838−2850

cases, their luminescence properties at ambient temperature. Several of these complexes include additional metal ions from the 3d block series, and their magnetic properties are also described.

EXPERIMENTAL SECTION

Syntheses. ***Caution!*** *Uranium is a radioactive and chemically toxic element, and uranium-containing samples must be handled with suitable care and protection.*

$UO_2(NO_3)_2{\cdot}6H_2O$ (depleted uranium, R. P. Normapur, 99%), $Co(NO_3)_2{\cdot}6H_2O$, and $Ni(NO_3)_2{\cdot}6H_2O$ were purchased from Prolabo, bipy was from Fluka, and $Cu(NO_3)_2{\cdot}2.5H_2O$ and 1,3-adamantanedicarboxylic acid (LH_2) were from Aldrich. All were used without further purification. Elemental analyses were performed by MEDAC Ltd. at Chobham, U.K.

*$[UO_2(L)(H_2O)]{\cdot}1.25CH_3CN$ (**1**).* LH_2 (11 mg, 0.05 mmol), $UO_2(NO_3)_2{\cdot}6H_2O$ (25 mg, 0.05 mmol), acetonitrile (0.3 mL), and demineralized water (0.7 mL) were placed in a 10 mL tightly closed glass vessel and heated at 140 °C under autogenous pressure, giving light yellow crystals of complex **1** within 4 d (17 mg, 61% yield). The acetonitrile molecules are lost upon washing with water and drying (and possibly some hydration occurs). Anal. Calcd for $C_{12}H_{16}O_7U$ (desolvated compound): C, 28.24; H, 3.16. Found: C, 27.06; H, 3.19%.

*$[UO_2(L)(DMF)]$ (**2**).* LH_2 (11 mg, 0.05 mmol), $UO_2(NO_3)_2{\cdot}6H_2O$ (25 mg, 0.05 mmol), $Ni(NO_3)_2{\cdot}6H_2O$ (15 mg, 0.05 mmol), *N*,*N*-dimethylformamide (DMF, 0.3 mL), and demineralized water (0.6 mL) were placed in a 10 mL tightly closed glass vessel and heated at 140 °C under autogenous pressure, giving light yellow crystals of complex **2** in low yield overnight, mixed with green crystals of $[Ni_2(HCOO)_4(H_2O)_4]$[10] (formate anions being generated in situ from DMF hydrolysis).

*$[H_2NMe_2]_2[(UO_2)_2(L)_3]{\cdot}1.5H_2O$ (**3**).* LH_2 (11 mg, 0.05 mmol), $UO_2(NO_3)_2{\cdot}6H_2O$ (25 mg, 0.05 mmol), DMF (0.2 mL), and demineralized water (0.4 mL) were placed in a 10 mL tightly closed glass vessel and heated at 140 °C under autogenous pressure, giving light yellow crystals of complex **3** within one week (14 mg, 63% yield based on the diacid). Anal. Calcd for $C_{40}H_{61}N_2O_{17.5}U_2$: C, 36.23; H, 4.64; N, 2.11. Found: C, 36.75; H, 4.41; N, 2.04%.

*$[UO_2(L)(NMP)]$ (**4**).* LH_2 (11 mg, 0.05 mmol), $UO_2(NO_3)_2{\cdot}6H_2O$ (25 mg, 0.05 mmol), *N*-methyl-2-pyrrolidone (NMP, 0.3 mL), and demineralized water (0.4 mL) were placed in a 10 mL tightly closed glass vessel and heated at 140 °C under autogenous pressure, giving light yellow crystals of complex **4** overnight (13 mg, 44% yield). Anal. Calcd for $C_{17}H_{23}NO_7U$: C, 34.53; H, 3.92; N, 2.37. Found: C, 34.67; H, 3.90; N, 2.35%.

*$[UO_2Co(L)_2(bipy)_2]{\cdot}0.5H_2O$ (**5**).* LH_2 (22 mg, 0.10 mmol), $UO_2(NO_3)_2{\cdot}6H_2O$ (25 mg, 0.05 mmol), $Co(NO_3)_2{\cdot}6H_2O$ (15 mg, 0.05 mmol), bipy (16 mg, 0.10 mmol), DMF (0.4 mL), and demineralized water (0.6 mL) were placed in a 10 mL tightly closed glass vessel and heated at 140 °C under autogenous pressure, giving orange crystals of complex **5** within 2 d (29 mg, 53% yield). Anal. Calcd for $C_{44}H_{45}CoN_4O_{10.5}U$: C, 48.27; H, 4.14; N, 5.12. Found: C, 48.26; H, 3.90; N, 5.09%.

*$[UO_2Ni(L)_2(bipy)_2]{\cdot}0.5H_2O$ (**6**).* LH_2 (11 mg, 0.05 mmol), $UO_2(NO_3)_2{\cdot}6H_2O$ (25 mg, 0.05 mmol), $Ni(NO_3)_2{\cdot}6H_2O$ (15 mg, 0.05 mmol), bipy (8 mg, 0.05 mmol), DMF (0.2 mL), and demineralized water (0.6 mL) were placed in a 10 mL tightly closed glass vessel and heated at 140 °C under autogenous pressure, giving light pink crystals of complex **6** within one week (14 mg, 51% yield based on the diacid). Anal. Calcd for $C_{44}H_{45}N_4NiO_{10.5}U$: C, 48.28; H, 4.14; N, 5.12. Found: C, 48.00; H, 3.74; N, 5.06%.

*$[Ni(bipy)_3][(UO_2)_4(O)_2(L)_3]{\cdot}3H_2O$ (**7**).* LH_2 (11 mg, 0.05 mmol), $UO_2(NO_3)_2{\cdot}6H_2O$ (25 mg, 0.05 mmol), $Ni(NO_3)_2{\cdot}6H_2O$ (15 mg, 0.05 mmol), bipy (8 mg, 0.05 mmol), acetonitrile (0.3 mL), and demineralized water (0.8 mL) were placed in a 10 mL tightly closed glass vessel and heated at 140 °C under autogenous pressure, giving orange crystals of complex **7** within two weeks (13 mg, 44% yield based on uranium). Anal. Calcd for $C_{66}H_{72}N_6NiO_{25}U_4$: C, 33.59; H, 3.07; N, 3.56. Found: C, 33.21; H, 3.04; N, 3.89%.

*$[UO_2Cu(L)_2]$ (**8**).* LH_2 (22 mg, 0.10 mmol), $UO_2(NO_3)_2{\cdot}6H_2O$ (25 mg, 0.05 mmol), $Cu(NO_3)_2{\cdot}2.5H_2O$ (12 mg, 0.05 mmol), acetonitrile (0.3 mL), and demineralized water (0.6 mL) were placed in a 10 mL tightly closed glass vessel and heated at 140 °C under autogenous pressure, giving blue-green crystals of complex **8** within one week (27 mg, 69% yield). Anal. Calcd for $C_{24}H_{28}CuO_{10}U$: C, 37.05; H, 3.63. Found: C, 36.82; H, 3.33%.

*$[(UO_2)_2Cu_2(L)_3(NO_3)_2(bipy)_2]{\cdot}0.5H_2O$ (**9**).* LH_2 (11 mg, 0.05 mmol), $UO_2(NO_3)_2{\cdot}6H_2O$ (25 mg, 0.05 mmol), $Cu(NO_3)_2{\cdot}2.5H_2O$ (12 mg, 0.05 mmol), bipy (8 mg, 0.05 mmol), acetonitrile (0.3 mL), and demineralized water (0.8 mL) were placed in a 10 mL tightly closed glass vessel and heated at 140 °C under autogenous pressure, giving dark green crystals of complex **9** within 3 d (25 mg, 84% yield based on the diacid). The same complex is obtained when acetonitrile is replaced by tetrahydrofuran (THF). Anal. Calcd for $C_{56}H_{59}Cu_2N_6O_{22.5}U_2$: C, 37.80; H, 3.34; N, 4.72. Found: C, 38.00; H, 3.54; N, 4.87%.

Crystallography. The data were collected at 150(2) K on a Nonius Kappa-CCD area detector diffractometer[11] using graphite-monochromated Mo Kα radiation (λ = 0.710 73 Å). The crystals were introduced into glass capillaries with a protective coating of Paratone-N oil (Hampton Research). The unit cell parameters were determined from 10 frames and then were refined on all data. The data (combinations of φ- and ω-scans with a minimum redundancy of four (three for complex **3**, eight for complex **9**) for 90% of the reflections) were processed with HKL2000.[12] Absorption effects were corrected empirically with the program SCALEPACK.[12] The structures were solved either by usual direct methods with SHELXS[13] or by intrinsic phasing with SHELXT,[14] expanded when necessary by subsequent difference Fourier synthesis and refined by full-matrix least-squares on F^2 with SHELXL.[13] All non-hydrogen atoms were refined with anisotropic displacement parameters. The hydrogen atoms bound to oxygen atoms were found on difference Fourier maps, except when indicated below. The carbon-bound hydrogen atoms were introduced at calculated positions in all compounds. All hydrogen atoms were treated as riding atoms with an isotropic displacement parameter equal to 1.2 times that of the parent atom (1.5 for CH_3). Special details are as follows.

*Complex **1**.* One acetonitrile solvent molecule is disordered around an inversion center, and it was given an occupancy factor of 0.5.

*Complex **3**.* Restraints on displacement parameters were needed for some atoms that became too strongly anisotropic during refinement. The hydrogen atoms of the solvent water molecules were neither found nor introduced; those bound to nitrogen atoms were introduced at calculated positions.

*Complexes **5** and **6**.* The oxygen atom of the water solvent molecule was given an occupancy factor of 0.5 to retain an acceptable displacement parameter, and its hydrogen atoms were found on a difference Fourier map.

*Complex **7**.* Some water solvent molecules were given partial occupancies to retain acceptable displacement parameters and/or to allow for too-close contacts, and some of them had to be refined with restraints on displacement parameters. The hydrogen atoms were found for only one of these water molecules.

*Complex **9**.* The water solvent molecule was given an occupancy factor of 0.5 to retain an acceptable displacement parameter, and its hydrogen atoms were neither found nor introduced. The highest residual electron density peak is located at 0.95 Å from atom U2, and it may result either from imperfect absorption corrections or from a minor disordered component of atom U2. However, in the latter case, the corresponding disordered positions of the coordinated oxygen atoms were not found, and it was deemed better not to introduce the minor U2 component.

Crystal data and structure refinement parameters are given in Table 1. The molecular plots were drawn with ORTEP-3,[15] and the polyhedral representations were drawn with VESTA.[16] The topological analyses were done with TOPOS.[17]

DOI: 10.1021/ic503004j
Inorg. Chem. 2015, 54, 2838−2850

Luminescence Measurements. Emission spectra were recorded at ~298 K on solid samples using a Horiba-Jobin-Yvon Fluorolog spectrofluorimeter. Powdered complex was pressed between two silica plates, which were mounted such that the faces were oriented vertically and at 45° to the incident excitation radiation. An excitation wavelength of 420 nm was used in all cases, and the emissions were monitored between 450 and 650 nm.

Magnetic Measurements. Magnetic measurements on powder samples were carried out with a Quantum Design SQUID Magnetometer with an applied field of 1000 G. The independence of the susceptibility value with regard to the applied field was checked at room temperature. The susceptibility data were corrected for the sample holder and the diamagnetic contributions as calculated from tables of Pascal's constants.

RESULTS AND DISCUSSION

Synthesis. The previously reported uranyl complex with L^{2-}, $[UO_2(L)(H_2O)]\cdot H_2O$, was synthesized in water at 180 °C from uranyl acetate dihydrate in the presence of a slight excess of ammonium acetate.[9] To screen more thoroughly the possible outcomes of the reaction of uranyl with this ligand, we performed a series of crystallization attempts under solvo-hydrothermal conditions at 140 °C (no other temperature was used) with either acetonitrile, DMF, NMP, THF, or methanol as organic cosolvents. In each case, the reaction was conducted either with uranyl nitrate alone, or with additional cobalt(II), nickel(II), or copper(II) nitrate, the latter cations being added in view of increasing the assembly dimensionality.[1c,2p,q,18] For each of the 3d block cations, attempts were made with or without addition of bipy, a ligand with a strong affinity for these cations. No basic agent was added in any case (except bipy as just stated, but in view of its coordinating properties), since they are not necessary for the complete deprotonation of the diacid under the present conditions. All crystals were grown during the heating phase (not upon cooling), and their presence in the glass vials was checked visually.

Most of these experiments did not produce crystals suitable for diffraction, common outcomes being the formation of amorphous or microcrystalline precipitates, or of no solid whatever, even after heating had been continued for several weeks. Methanol and THF appeared particularly unsuitable in this respect. Among the nine complexes that could be crystallographically characterized, four were obtained with each of acetonitrile (**1** and **7**–**9**) and DMF (**2**, **3**, **5**, and **6**), while only one involved NMP (**4**). This last case is quite interesting since this complex, with NMP being present as a coligand, was crystallized in most experiments with this solvent, even in the presence of additional cations, thus indicating the particular stability of this species. DMF is the only one among these solvents to be unstable under the conditions used and to be readily hydrolyzed into formic acid and dimethylamine;[19] as a result, nickel formate was formed alongside complex **2**, and dimethylammonium cations are found in complex **3**. From a general viewpoint, apart from their usefulness for enhancing the solubility of the reactants when this is necessary (and this particularly when no deprotonating agent is used, as in the present series),[20] water–organic solvent mixtures seem to provide a means for preventing in some measure the formation of uranyl oxo/hydroxo oligomeric species resulting from hydrolysis,[7,18k,21] which is widespread in uranyl aqueous chemistry.[1,22] Only one complex in the present series (**7**, obtained with acetonitrile as a cosolvent and the basic bipy as a coligand) contains additional oxo anions.

Crystal Structures. The complexes $[UO_2(L)(H_2O)]\cdot 1.25CH_3CN$ (**1**) and $[UO_2(L)(DMF)]$ (**2**) will be very briefly described since the first is only a different solvate of the complex previously reported,[9] while the second displays the same overall arrangement, with the aqua ligand replaced by a DMF molecule (Figure 1; additional views are given as

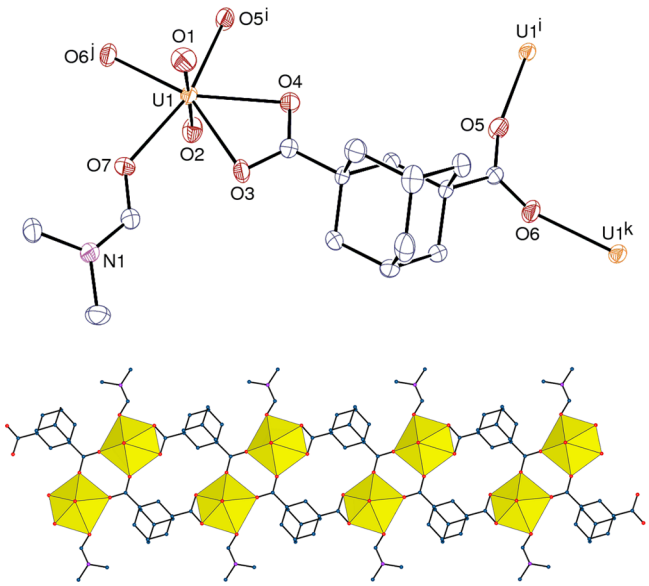

Figure 1. (upper) View of complex **2**. Displacement ellipsoids are drawn at the 50% probability level. Symmetry codes: i = 1 − *x*, 1 − *y*, 1 − *z*; j = *x* + 1, *y*, *z* + 1; k = *x* − 1, *y*, *z* − 1. (lower) View of the 1D assembly showing the uranium coordination polyhedra. Hydrogen atoms are omitted in both views.

Supporting Information). In both cases, the uranium atom is in the usual pentagonal bipyramidal coordination environment, with unexceptional bond lengths and angles, and the dicarboxylate ligand is both chelating and bridging bidentate, giving rise to the formation of a 1D coordination polymer with the point (Schläfli) symbol $\{4^2.6\}$. It is notable that the closely related 1,3-cyclohexanedicarboxylate ligand, although bound through the same chelating/bridging mode, yields either a 2D network or a ladderlike 1D polymer very different from the present one.[3] It may well be that the greater bulkiness of the adamantane-derived ligand plays a part in preventing such arrangements. Indeed, in both **1** and **2**, the adamantane skeletons bulge on the outside of the chains.

Complex **3**, $[H_2NMe_2]_2[(UO_2)_2(L)_3]\cdot 1.5H_2O$, obtained with DMF as a cosolvent, and thus in the presence of dimethylammonium cations generated in situ, is a completely different species. The crystal structure was solved and refined in the triclinic space group *P*1, with four independent uranyl ions and six L^{2-} ligands in the asymmetric unit, and there is no indication of a missed inversion center. All the uranyl ions are chelated by three carboxylate groups pertaining to three ligands, and the uranium atoms are in hexagonal bipyramidal environments, with U–O(carboxylate) bond lengths in the range of 2.407(8)–2.557(8) Å [average 2.47(4) Å] (Figure 2). Each metal cation is thus a 3-fold node, whereas the ligand is a 2-fold node only. Quite surprisingly, this connectivity mode gives rise to the formation of a 3D framework, with the total point symbol $\{20^3\}_2\{20\}_3$ (first symbol for uranium, second for the ligand; a nodal representation is given as Supporting Information). When viewed down the *c* axis, the structure

DOI: 10.1021/ic503004j
Inorg. Chem. 2015, 54, 2838–2850

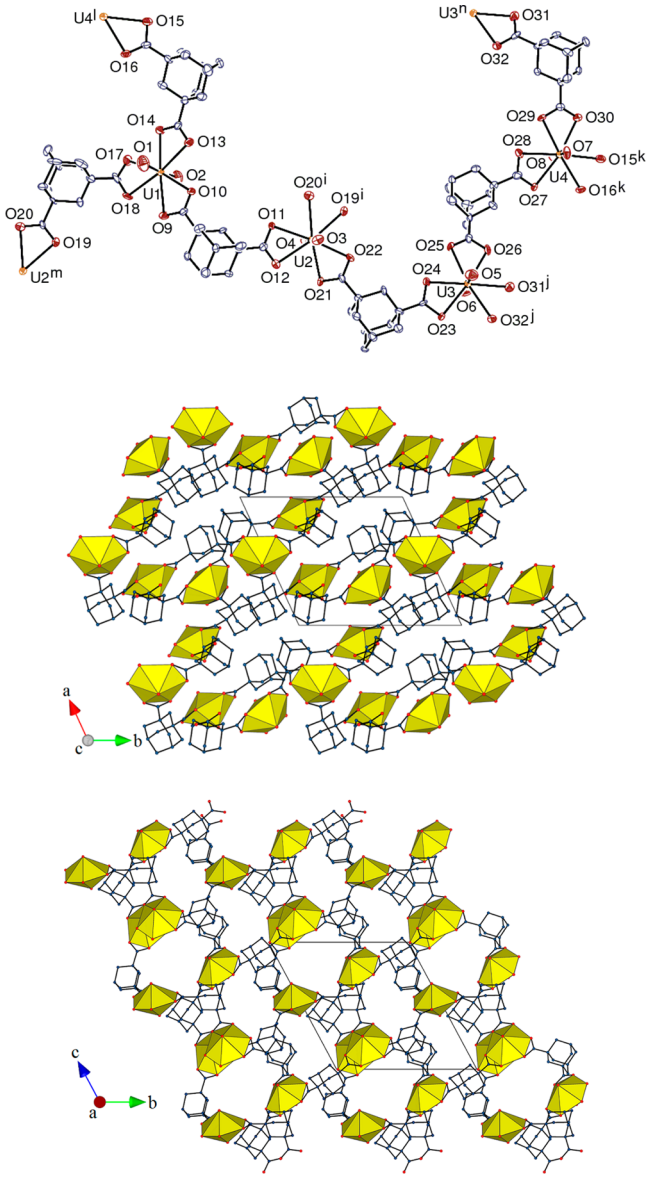

Figure 2. (upper) View of complex **3**. Displacement ellipsoids are drawn at the 50% probability level. Symmetry codes: i = *x*, *y* − 1, *z* − 1; j = *x* + 1, *y* + 1, *z*; k = *x*, *y* − 1, *z* − 2; l = *x*, *y* + 1, *z* + 2; m = *x*, *y* + 1, *z* + 1; *n* = *x* − 1, *y* − 1, *z*. (middle, lower) Two views of the 3D framework showing the uranium coordination polyhedra. Counterions, solvent molecules, and hydrogen atoms are omitted in all views.

displays elongated and very narrow channels, somewhat crescent-shaped in cross-section, with an approximate length of 20 Å, into which the adamantane carbon skeletons protrude (Figure 2, middle). Two different kinds of wider and more cylindrical channels appear in a view down the *a* axis, with approximate cross-sectional areas of 7 × 6 and 5 × 4 $Å^2$ for the larger and smaller ones, respectively (Figure 2, lower). These channels are occupied by the dimethylammonium counterions, which are hydrogen-bonded to either uranyl oxo groups, carboxylate oxygen atoms, or solvent water molecules, and may exert a structure-directing effect during the formation of the framework. With the counterions and solvent molecules excluded, the Kitaigorodski packing index (KPI, estimated with PLATON[23]) is 0.57.

The last complex with uranyl ions alone, $[UO_2(L)(NMP)]$ (**4**), includes NMP as a coligand, a common occurrence with this solvent.[7a,8,18k,21] The asymmetric unit contains two independent uranyl ions in similar environments (Figure 3). Each of them is bound to one chelating carboxylate group, two oxygen atoms from two different carboxylate ligands, and the NMP molecule. The U−O bond lengths are in the ranges of 2.407(3)−2.478(3) Å [average 2.45(3) Å] and 2.306(4)−2.399(3) Å [average 2.35(3) Å] for chelating and bridging bidentate donors, respectively. The U−O(NMP) bond lengths of 2.342(3) and 2.372(3) Å are within the range previously determined, 2.325(3)−2.438(6) Å. As in complexes **1** and **2**, the ligands are both chelating and bridging bidentate, the latter coordination mode subtending the formation of uranyl dimers. However, each dimer is not connected to two neighbors, as in **1** and **2**, but to three, two of them on either direction along the chain axis, and the third in an oblique direction, as is apparent from comparison of the nodal representations of the two assemblies shown in Figure 4. As a result, the chains in **4** are braid-shaped and form a central channel occupied by the methyl groups of some of the NMP molecules (Figure 3, lower). The uranyl ions are located inside, and the outer surface is coated by the hydrophobic adamantyl framework and NMP molecules, a trend previously observed with closed species (cages or nanotubules) involving uranyl ions and Kemp's triacid.[7] The two uranium atoms are inequivalent nodes in the network, as well as the two L^{2-} ligands, each term in the total point symbol $\{4.8.10\}\{4^2.6\}$ corresponding to both one metal and one ligand. The packing of the chains leaves no free space, and the estimated KPI is 0.68.

The two isomorphous heterometallic complexes $[UO_2M(L)_2(bipy)_2]\cdot 0.5H_2O$ with M = Co (**5**) and Ni (**6**) were obtained in water/DMF. The asymmetric unit corresponds to the formula unit, both metal atoms being in general position (Figure 5). The uranium atom is chelated by three carboxylate groups, with U−O bond lengths in the range of 2.401(3)−2.514(2) Å [average 2.47(3) Å, for both compounds]. One of the bis-chelating ligands bridges two uranium atoms related to one another by the glide plane orthogonal to the *b* axis, while the other bridges uranium and 3d metal cations. The latter are also chelated by two bipy molecules, which gives an octahedral *cis*-N_4O_2 environment, distorted due to the small bite angle of the ligands. The average M−O and M−N bond lengths [respectively, 2.137(3) and 2.107(9) Å for Co; 2.10(2) and 2.061(13) Å for Ni] are unexceptional. Uranyl-containing chains parallel to the *c* axis are formed, with the $M(L)(bipy)_2$ groups attached to one side, with a tilt between successive units due to steric hindrance, so that, when viewed along the chain axis, the assembly appears to contain two slightly divergent appendages (Figure 5, middle). The chains are stacked in a head-to-tail fashion along both the *a* and *b* axes, and the packing has an estimated KPI value of 0.65 (solvent excluded). The 3d block metal cations have no part in the building of the polymer and can be viewed as decorating groups, just a step away from dissociation as counterions.

Such dissociation is achieved in complex **7**, $[Ni(bipy)_3][(UO_2)_4(O)_2(L)_3]\cdot 3H_2O$, which was obtained from the same reactants as complex **6** but in water/acetonitrile. This is the only case in the present series in which oxo anions are present as additional ligands. The asymmetric unit corresponds to the formula unit, all metal atoms being in general position (Figure 6). The four uranium atoms are connected through chelating, chelating and bridging, or bridging bidentate ligands, and they are assembled into two μ_3-oxo-bridged tetranuclear subunits, a very common uranyl secondary building unit (SBU).[1e,7b,19h,j,24]

DOI: 10.1021/ic503004j
Inorg. Chem. 2015, 54, 2838−2850

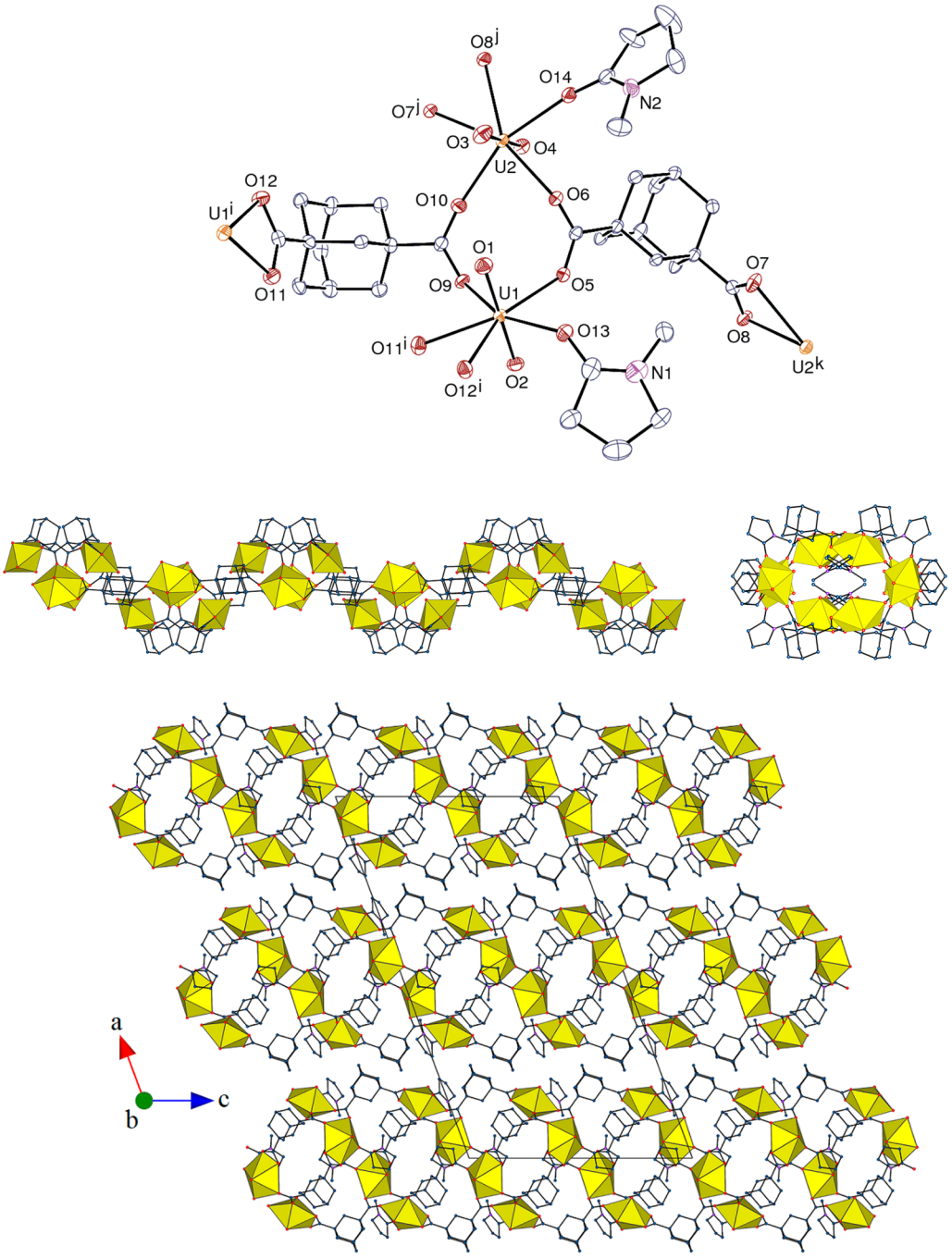

Figure 3. (upper) View of complex **4**. Displacement ellipsoids are drawn at the 30% probability level. Symmetry codes: i = 2 − *x*, *y*, 3/2 − *z*; j = *x*, 2 − *y*, *z* + 1/2; k = *x*, 2 − *y*, *z* − 1/2. (middle) Two views of the 1D assembly, edge-on (left) or end-on (right). (lower) View of the packing. Hydrogen atoms are omitted in all views.

Each uranyl ion is chelated by one carboxylate group [U−O bond lengths in the range of 2.419(3)−2.592(3) Å, average 2.50(6) Å; the values corresponding to the bridging oxygen atoms O9 and O11 being larger than the others by ∼0.1 Å]. The pentagonal bipyramidal environment of each uranium atom is completed by either one monodentate carboxylate and two oxo anions (U1 and U3) or by two carboxylate oxygen atoms (one from a chelating group) and one oxo anion (U2 and U4). The corresponding U−O(carboxylate) and U−O(oxo) bond lengths are in the ranges of 2.336(3)−2.448(3) Å [average 2.39(4) Å] and 2.229(3)−2.278(3) Å [average 2.255(17) Å]. These tetranuclear SBUs, with all uranium atoms seven-coordinated, correspond to the most common type, denoted (*i*) in the recent review of Loiseau et al.[1e] The L^{2-} ligands bridge these SBUs to give a 2D assembly parallel to (1 0 $\bar{1}$) with the total point symbol $\{4^2.6\}_2\{4^2.8^2.10^2\}$-$\{4^3.6^2.8\}_4\{4^3\}_2$ (successive symbols for two L^{2-} ligands, one L^{2-} ligand, the four uranium atoms, and the two oxo anions). When viewed down the *b* axis, these sheets display a triangular wave shape with the adamantyl groups marking the turning points. The $Ni(bipy)_3^{2+}$ cations are located in the large intersheet channels (∼16 × 9 Å) directed along the *b* axis (Figure 6, lower).

DOI: 10.1021/ic503004j
Inorg. Chem. 2015, 54, 2838−2850

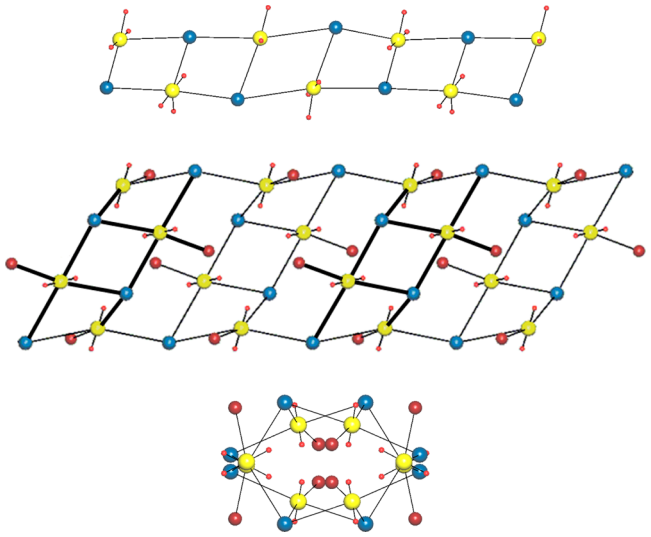

Figure 4. Nodal representation of the 1D assemblies in **1** (upper) and **4** (middle), and the latter viewed down the chain axis (lower). Yellow: uranium, red: oxygen, blue: centroid of the dicarboxylate ligand, dark red: centroid of NMP. The bonds to nodes located upward are in bold lines in the middle view.

The last two compounds, namely, $[UO_2Cu(L)_2]$ (**8**) and $[(UO_2)_2Cu_2(L)_3(NO_3)_2(bipy)_2]\cdot 0.5H_2O$ (**9**), were obtained in the presence of copper nitrate in water/acetonitrile, with additional bipy ligands in the second case. The asymmetric unit in **8** corresponds to half the formula unit, with the uranium atoms located on an inversion center (Wyckoff position 4*a* of space group *C*2/*c*) and the copper atoms on a 2-fold rotation axis (position 4*e*). Unusually, the uranium atom is in a tetragonal bipyramidal environment, being bound to four carboxylate oxygen atoms from four different ligands in its equatorial plane (Figure 7), with U−O(carboxylate) bond lengths of 2.306(3) and 2.309(3) Å, shorter than in the other compounds due to the reduced coordination number, and in good agreement with the average bond length of 2.28(6) Å for this geometry calculated for similar structures in the Cambridge Structural Database (CSD, 2014 release, Version 5.35; 76 hits with oxygen or nitrogen donors).[25] The copper atom is bound to four carboxylate oxygen atoms and is in a very distorted square planar environment [Cu−O bond lengths of 1.926(3) and 1.944(3) Å, root-mean-square deviation from the mean plane 0.43 Å]. Both metal atoms are thus 4-fold nodes, as well as the ligand, which is doubly bridging bidentate. This connectivity results in the building of a 3D framework with the total point symbol $\{4^2.8^2.10^2\}\{4^3.6^2.8\}_2\{4^4.6^2\}$ (successive symbols for uranium atoms, ligands, and copper atoms), which is represented in nodal form in Figure 8. The uranium atoms and ligands alone are assembled into 2D $UO_2(L)_2$ subunits parallel to $(1\ 0\ \bar{1})$, whereas the copper atoms and ligands alone give $Cu(L)_2$ chains directed along the [1 0 1] direction, so that both cations are needed in the building of the framework. Alternate layers of ligands and metal cations run parallel to the *bc* plane. No significant free space is present in the lattice, as shown by the estimated KPI of 0.70.

The asymmetric unit in complex **9** corresponds to the formula unit, with all metal atoms in general position and the two uranium atoms in different environments (Figure 9). U1 is bound to four carboxylate oxygen atoms from four L^{2-} ligands [U−O bond lengths in the range of 2.315(8)−2.357(6) Å, average 2.344(17) Å] and one chelating nitrate ion, thus giving a uranium coordination number of eight, with the particularity that the ONO chelating site is parallel to the uranyl axis. This very unusual arrangement has previously been observed in a few cases, with only one of them corresponding to an overall coordination number of eight.[26] The nitrate bonding is quite asymmetrical, with U1−O(nitrate) bond lengths of 2.530(7) and 2.881(11) Å for O17 and O18, respectively [2.518(7) and 2.691(7) Å in the previous case]; the uranium atom and the four carboxylate donors define a mean plane with a root-mean-squares deviation of 0.02 Å, which makes a dihedral angle of 86.2(5)° with the ONO plane. The distances of O17, O18, and N1 from this mean plane are 1.030(10), −1.055(12), and 0.071(13) Å, respectively, showing that the nitrate group straddles the uranyl equatorial plane. Consequently, the O1−U1−O2 angle of 172.9(3)° reflects some departure from linearity, with the two oxo groups being pushed away from the nitrate group. The coordination polyhedron of U1 is thus a pentagonal bipyramid with a split equatorial vertex. Atom U2 is chelated by two carboxylate groups and one nitrate ion, with a hexagonal bipyramidal environment. The U−O(carboxylate) bond lengths are in the range of 2.431(7)−2.464(7) Å [average 2.447(12) Å], and the U−O(nitrate) bond lengths are 2.525(7) and 2.542(7) Å. The copper atoms are bound to two carboxylate oxygen atoms from different ligands and one chelating bipy molecule, which gives a square planar environment [bond lengths in the range of 1.931(6)−2.009(9) Å], and they make a longer axial contact with oxo groups pertaining to the same uranyl ion [Cu1−O1 2.400(6), Cu2−O2 2.418(6) Å], resulting in an axially elongated square pyramidal geometry. Such so-called (however improperly) cation−cation interactions involving d block cations are quite frequent in uranyl chemistry.[1,2p,7b,18a,e,g,h,l,21,27] The Cu−O(oxo) bond lengths in **9** are in the lower range of usual values (2.40−2.75 Å), but shorter ones (about 2.2 Å) have recently been found.[27g] It is notable that the U═O bond lengths involving the bridging oxo atoms O1 and O2, 1.788(6) and 1.794(6) Å, respectively, are slightly larger than usual [for example, 1.742(7) and 1.756(7) Å for atom U2]. Two dicarboxylate ligands are chelating/bridging bidentate, and the third is doubly bridging bidentate; all the bridging groups connect uranium and copper atoms. The resulting 1D assembly is directed along $[0\ 1\ \bar{1}]$ and has the total point symbol of $\{4.8^2\}_2\{4^2\}\{4^6\}\{4\}_2\{8\}$ (successive symbols for two L^{2-} ligands, atom U1, the third ligand, the two copper atoms, and atom U2). From a geometrical viewpoint, uranium atoms alone are sufficient to account for the formation of the polymer (Figure 9, lower). As in compounds **5** and **6**, the terminating nature of the bipy ligand prevents the Cu(bipy) group from being an efficient linker. As in complex **4**, the chains appear to be somewhat inflated when viewed end-on. No significant free space is present in the packing (KPI = 0.65, with solvent excluded).

Luminescence Properties. Emission spectra under excitation at a wavelength of 420 nm in the solid state were recorded for all compounds except **2**, for which a sufficient amount of pure crystals could not be isolated. Representative spectra are given in Figure 10 (and the others are given as Supporting Information). Where transition metal ion centers are absent, the solids presently isolated show well-resolved luminescence typical of uranyl ion.[28] The usual vibronic progression in the ∼460−600 nm range is apparent in the spectra of compounds **3** and **4**, and also in **1**, although in the latter case the intensity is reproducibly very low, with six peaks

DOI: 10.1021/ic503004j
Inorg. Chem. 2015, 54, 2838−2850

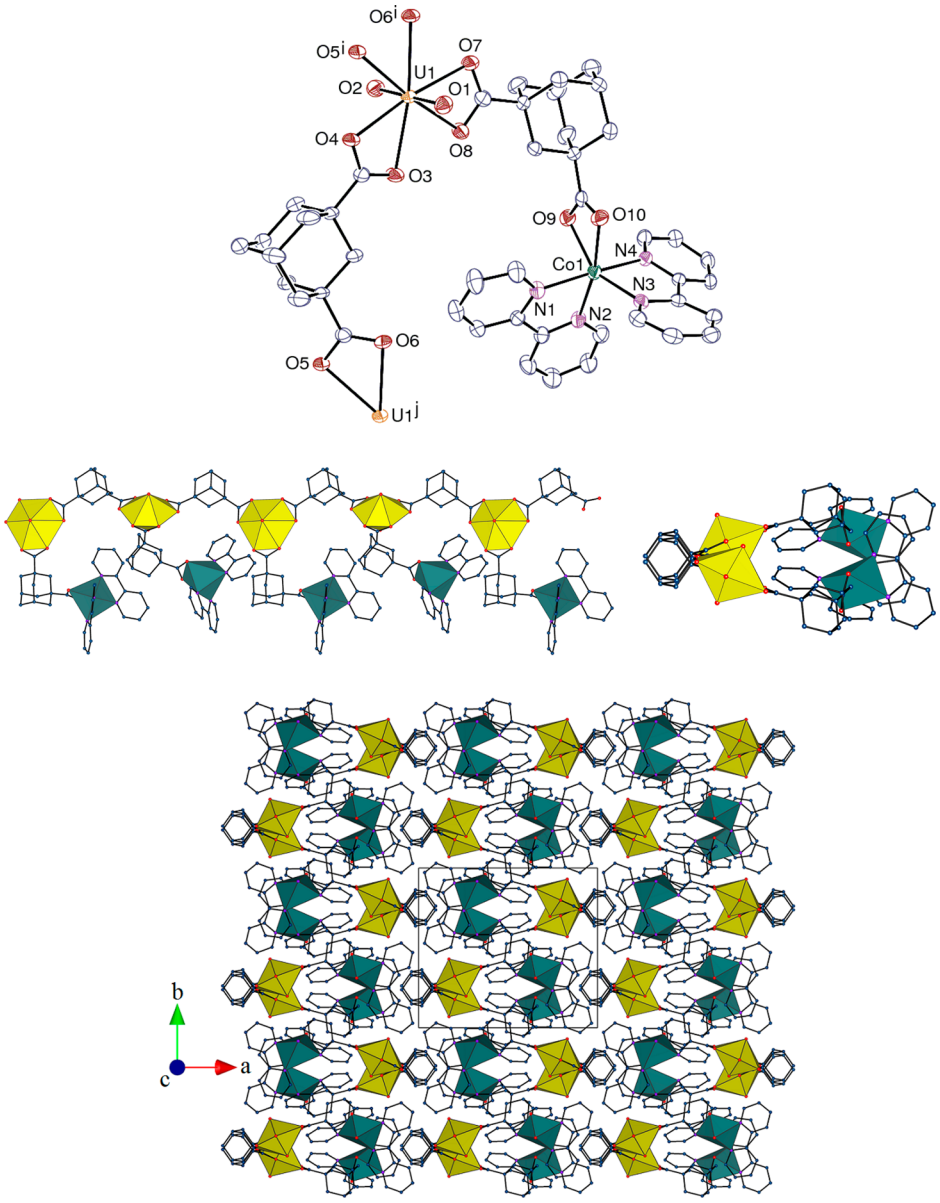

Figure 5. (upper) View of complex **5**. Displacement ellipsoids are drawn at the 50% probability level. Symmetry codes: i = x, $1/2 - y$, $z + 1/2$; j = x, $1/2 - y$, $z - 1/2$. (middle) Two views of the 1D assembly, edge-on (left) or end-on (right). (bottom) View of the packing. The uranium coordination polyhedra are shown in yellow, and those of cobalt are shown in green. Solvent molecules and hydrogen atoms are omitted in all views.

corresponding to the $S_{11} \rightarrow S_{00}$ and $S_{10} \rightarrow S_{0\nu}$ (ν = 0−4) electronic transitions.[29] The positions of the three major peaks vary significantly, with a shift of ca. 11−14 nm when going from **3** (480, 500, and 522 nm) to **4** (491, 513, and 536 nm). This is probably due to the variation in the number of donor atoms in the equatorial plane of the uranium coordination sphere, six in **3** and five in **4**, a factor which is known to affect the band positions.[30] Transition metal ions, Cu(II) in particular, are known to be quenchers of uranyl ion emission, due to energy transfer to the d−d absorption band and nonradiative decay, and this is observed for complexes **5**, **8**, and **9**, which are essentially nonluminescent, as is the case in some closely related species.[8,18k,21,31] However, such quenching is not always complete, as shown by the well-resolved (but rather weak) emission observed for the Ni(II)-containing species **6**. In the presence of Ni(II) as $[Ni(bipy)_3]^{2+}$ in complex **7**, while the uranyl emission is quenched, a new, very broad emission band appears, with three barely resolved maxima in the 515−542 nm range. In both its form and position, this band corresponds well with the $^3A_{2g} \rightarrow {}^3T_{1g}$ absorption band observed near 520 nm in the solution (ethanol) spectrum of $[Ni(bipy)_3](ClO_4)_2$.[32] Since excitation of $[Ni(bipy)_3](NO_3)_2$ at the same wavelength (420 nm) as used for the uranyl-containing species produces no emission near 530 nm, it would appear that the excited uranyl unit is able to transfer its energy of excitation directly to the $^3T_{1g}$ excited state of the Ni(II) center, which then undergoes a radiative decay. This also appears to be the case in the heterometallic complex $[(UO_2)_2Ni(nta)_2(NMP)_2]\cdot NMP$ (nta = nitrilotriacetate).[18k] The energy transfer luminescence seen with Ni(II) is completely analogous to that from U(VI) to Sm(III) found in the mixed uranyl ion/samarium(III) complex of phosphonoacetic acid,[33] where again there is a close proximity of the excited-state energies. For these mixed uranyl−lanthanide phosphonoacetates, where the energy match is poor, as in the U(VI)−Tb(III) complex, energy

DOI: 10.1021/ic503004j
Inorg. Chem. 2015, 54, 2838−2850

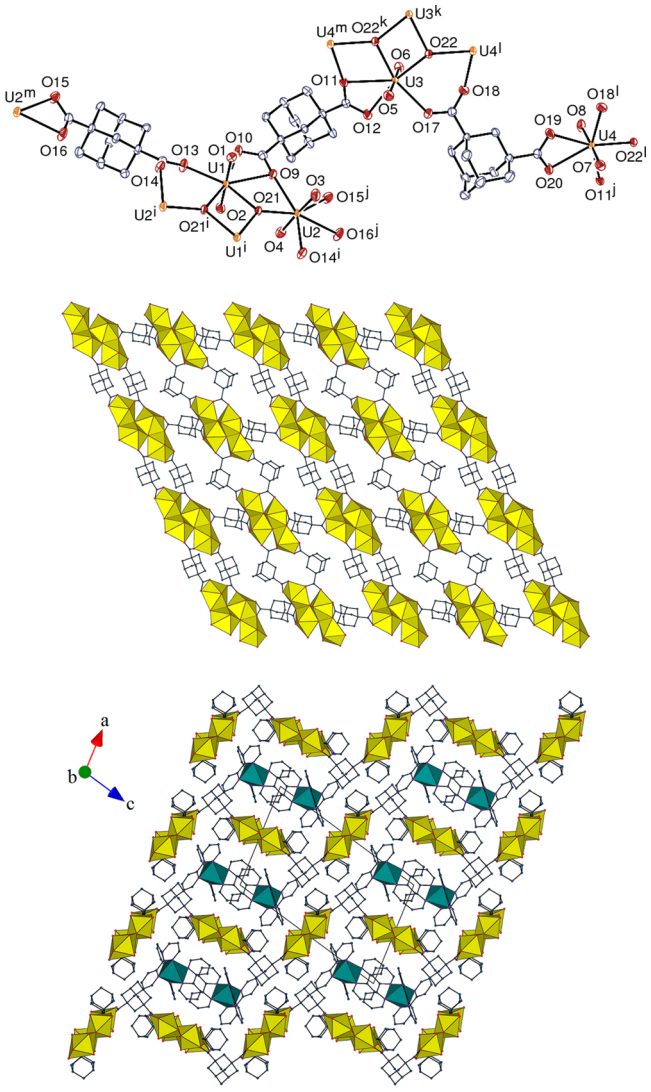

Figure 6. (upper) View of complex **7**. Counterions, solvent molecules, and hydrogen atoms are omitted. Displacement ellipsoids are drawn at the 50% probability level. Symmetry codes: i = −*x*, −*y*, 1 − *z*; j = *x*, *y* − 1, *z*; k = 1 − *x*, −*y*, 2 − *z*; l = 1 − *x*, −*y* − 1, 2 − *z*; m = *x*, *y* + 1, *z*. (middle) View of the 2D assembly. (lower) View of the packing with sheets edge-on. The uranium coordination polyhedra are shown in yellow, and those of nickel are shown in green.

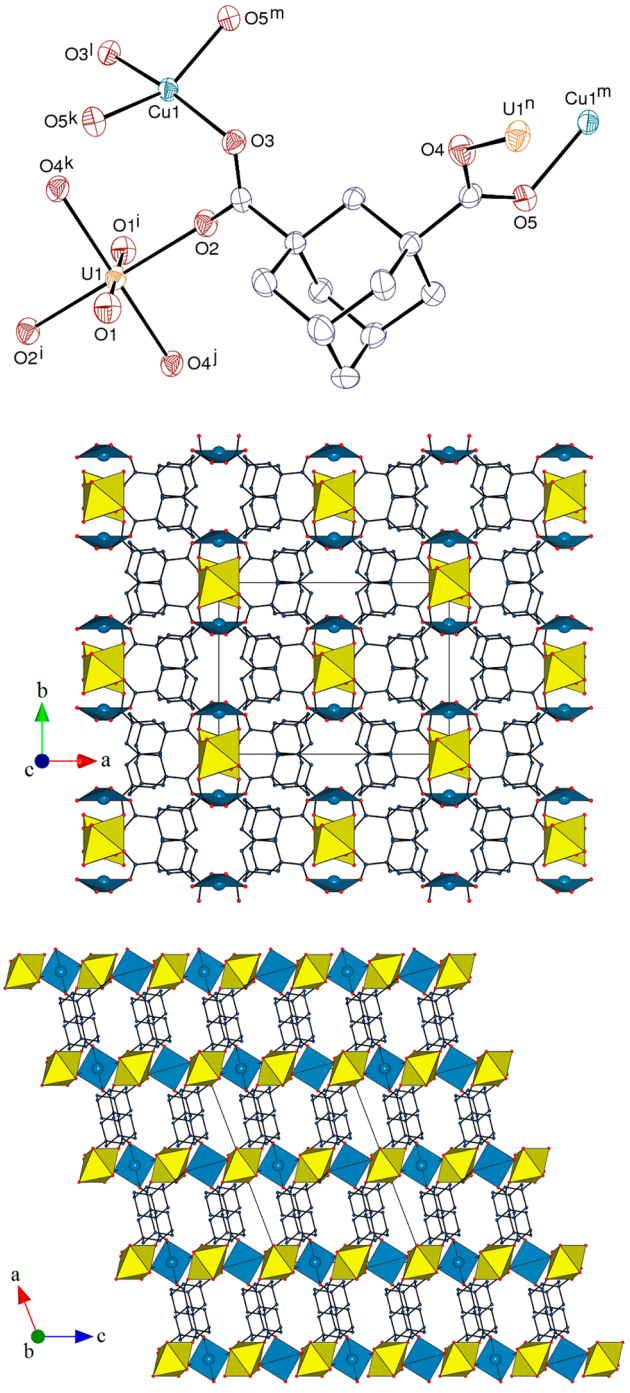

Figure 7. (upper) View of complex **8**. Displacement ellipsoids are drawn at the 50% probability level. Symmetry codes: i = 1 − *x*, 1 − *y*, −*z*; j = 3/2 − *x*, *y* + 1/2, 1/2 − *z*; k = *x* − 1/2, 1/2 − *y*, *z* − 1/2; l = 1 − *x*, *y*, 1/2 − *z*; m = 3/2 − *x*, 1/2 − *y*, 1 − *z*; *n* = 3/2 − *x*, *y* − 1/2, 1/2 − *z*. (middle, lower) Two views of the 3D framework. The uranium coordination polyhedra are shown in yellow, and those of copper are shown in blue. Hydrogen atoms are omitted in all views.

transfer does not occur, and the normal uranyl luminescence is observed. This is also seen for a mixed U(VI)−Ni(II) complex where the Ni is present as the aqua-complex $[Ni(H_2O)_6]^{2+}$,[8] and indeed in the present case of complex **6** where uranyl emission, although relatively weak, is seen, consistent with the fact that the N_4O_2 coordination environment here would lower the ligand field and hence place the $^3A_{2g} \rightarrow {}^3T_{1g}$ transition more remote from the uranyl band. The complete quenching of uranyl emission seen in the present mixed U/Co (**5**) and U/Cu (**8**, **9**) complexes is consistent with energy transfer being followed by nonradiative energy loss, as suggested in other cases.[21,31c] For the present Cu(II) species in particular, given that uranyl ion is a known photo-oxidant[28,30,34] and that bipyridine stabilizes the +I oxidation state of Cu, this is more probable than that the quenching of the uranyl luminescence by the Cu(II) centers is due to photoinduced electron transfer[35] giving a U(V)−Cu(III) pair. Note that, while quenching of uranyl luminescence by Cu(II) is commonly observed, it is not always complete[31c] and that any such effects are not necessarily associated with the presence of d−d excited states, as shown by the presence[31c] and absence[36] of quenching in different mixed U(VI)−Ag(I) complexes.

Magnetic Properties. Since uranyl is a diamagnetic cation, the magnetic properties were investigated only for the complexes containing additional paramagnetic d block cations (except for complex **7**, in which the paramagnetic ions are

DOI: 10.1021/ic503004j
Inorg. Chem. 2015, 54, 2838−2850

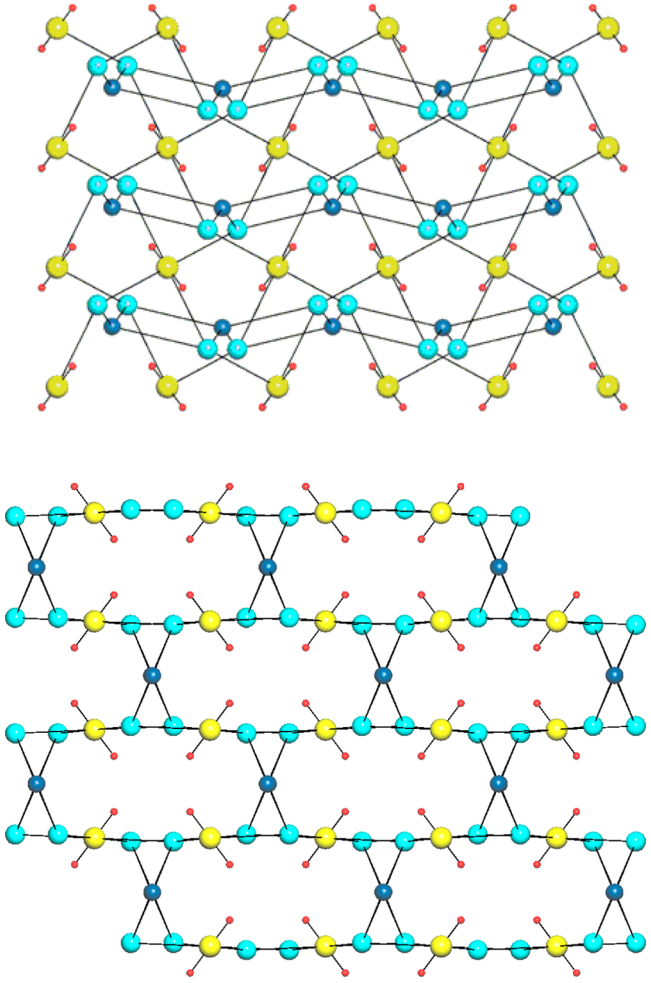

Figure 8. Nodal representation of the framework in **8** with *c* axis horizontal and *b* axis vertical (upper), and down the [1 0 1] axis with *b* axis horizontal, showing the uranium-containing sheets edge-on and the copper-containing chains end-on (lower). Yellow: uranium, dark blue: copper, red: oxygen, light blue: centroid of the dicarboxylate ligand.

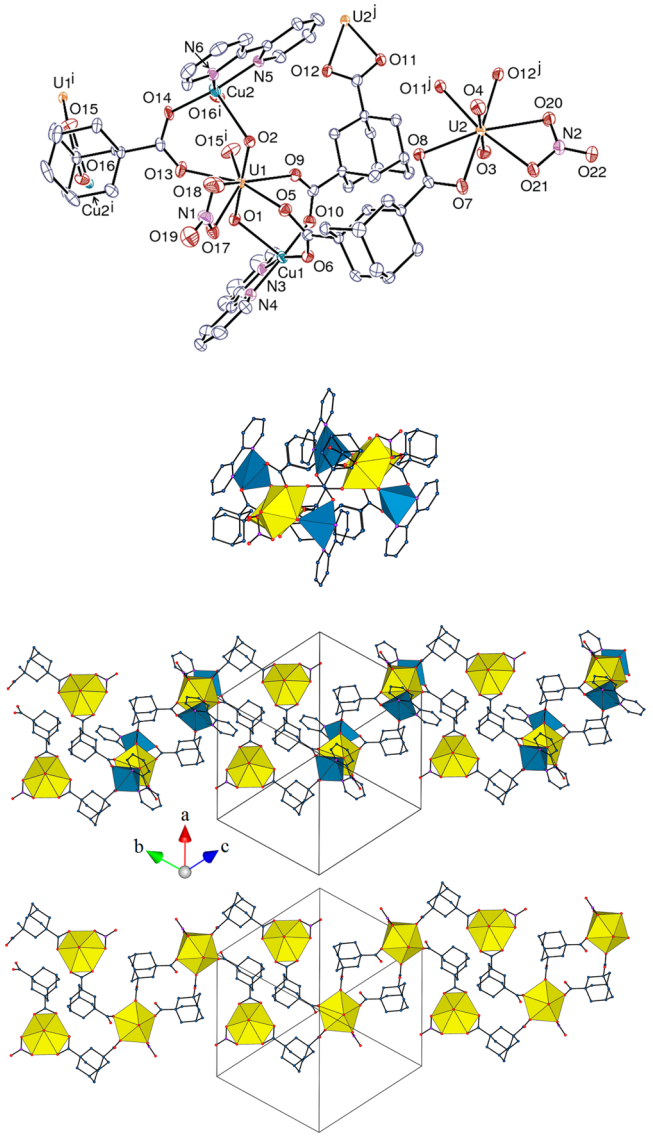

Figure 9. (upper) View of complex **9**. Displacement ellipsoids are drawn at the 30% probability level. Symmetry codes: i = 1 − *x*, 1 − *y*, 2 − *z*; j = 1 − *x*, 2 − *y*, 1 − *z*. (middle) View of the 1D assembly shown end-on. (lower) Two views of the 1D assembly, with and without copper atoms. The uranium coordination polyhedra are shown in yellow, and those of copper are shown in blue. Solvent molecules and hydrogen atoms are omitted in all views.

isolated within counterions). The temperature dependence of the product $\chi_M T$ (where χ_M is the molar susceptibility) in the 2−300 K range for the two isomorphous compounds **5** and **6** are given in Figures 11 and 12, respectively. In the case of the Co(II) complex **5**, the $\chi_M T$ curve slightly increases from 300 to 130 K and then decreases to 2.3 cm^3 mol^{-1} K at 5 K. The value of $\chi_M T$ at room temperature is larger than that expected for the spin-only case (1.875 for S = 3/2), suggesting the presence of a large orbital contribution.[37] The coordination octahedron around Co(II) is strongly distorted; attempts were made to fit the data with the empirical equation developed by Lloret et al.,[38] but no reasonable solution was found. In the case of the Ni(II) complex **6**, $\chi_M T$ is constant between room temperature and 30 K (1.13 cm^3 mol^{-1} K) and then decreases from 30 to 2 K. This decrease at low temperature can be attributed to the zero-field splitting effect[39] and possibly to antiferromagnetic intermolecular interactions. To investigate the magnitude of the local axial zero-field splitting parameter *D*, magnetization versus field curves recorded at 2, 4, and 6 K (Figure 12, inset) were fitted with the Hamiltonian

$$\mathbf{H} = \beta H \mathbf{g}\cdot\mathbf{S} + D[\mathbf{S}_z^{\,2} - 1/3\mathbf{S}(\mathbf{S}+1)] \qquad (1)$$

where β is the Bohr magneton, H is the magnetic field, **g** is the *g* tensor. The fitting process could not discriminate between positive or negative *D* values, the best fits giving either $D = -3.8$ cm^{-1} ($R = 5 \times 10^{-4}$ with $R = \sum(\chi_{cal}T - \chi_{exp}T)^2/\sum(\chi_{exp}T)^2$) or $D = +2.9$ cm^{-1} ($R = 4 \times 10^{-4}$), with $g = 2.13$ (the *g* value was previously determined by fitting the $1/\chi_M = f(T)$ curve with a Curie−Weiss law (see Supporting Information). The addition of an intermolecular parameter $\theta = -0.07$ K is needed to reproduce perfectly ($R = 4 \times 10^{-5}$) the $\chi_M T$ versus T curve with the above parameters (Figure 12).

The $\chi_M T$ versus T and M versus H plots (where M is the magnetization expressed in Bohr magneton) for the Cu(II) complex **8** are given as Supporting Information, and those for **9** are depicted in Figure 13. For **8**, the $\chi_M T$ value remains constant when the temperature varies from 300 to 2 K, with a value of 0.447 cm^3 mol^{-1} K, which is consistent with the

DOI: 10.1021/ic503004j
Inorg. Chem. 2015, 54, 2838−2850

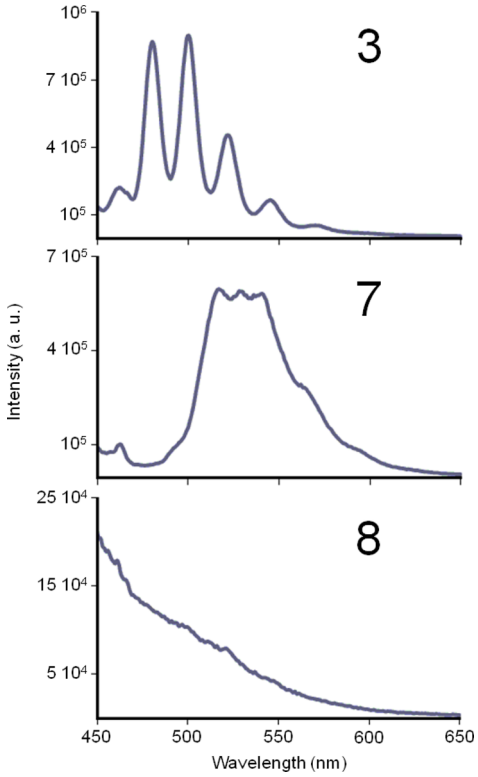

Figure 10. Solid-state emission spectra of complexes **3**, **7**, and **8**. Excitation wavelength 420 nm.

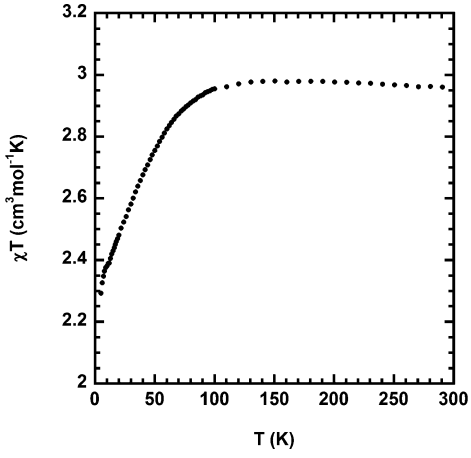

Figure 11. Plot of the temperature dependence of $\chi_M T$ for compound **5**.

magnetic behavior of isolated Cu(II) ions following the Curie law with g = 2.18. This is confirmed by the dependence of the magnetization on the magnetic field recorded at 2 K, which matches the Brillouin function for a spin of S = 1/2 and a g value of 2.18. These results are in agreement with the structure, in which there is no distance between copper ions shorter than 8.48 Å.

For complex **9**, the $\chi_M T$ value is constant and equal to 0.882 $cm^3\ mol^{-1}$ K when the temperature decreases from 300 to 20 K; then, it decreases slightly to 0.695 $cm^3\ mol^{-1}$ K at 2 K. The value of $\chi_M T$ at high temperature is consistent with two noninteracting Cu(II) ions ($\chi_M T$ = 0.750 $cm^3\ mol^{-1}$ K with g = 2), and the decrease at low temperature indicates the presence of weak antiferromagnetic interactions. The interaction

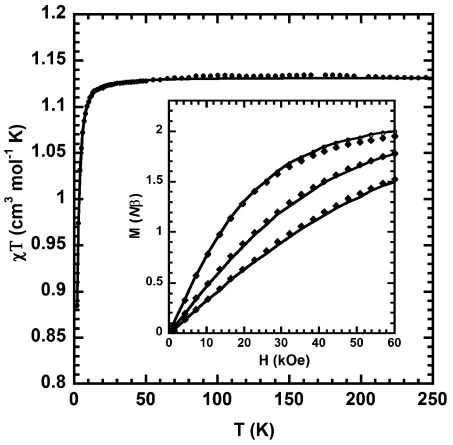

Figure 12. Plot of the temperature dependence of $\chi_M T$ for compound **6** (● experimental data, — best fit). (inset) Plot of the magnetization vs magnetic field at 2, 4, and 6 K (◆ experimental data, — best fit).

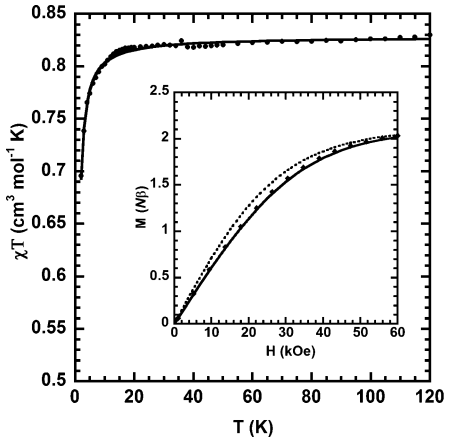

Figure 13. Plot of the temperature dependence of $\chi_M T$ for compound **9** (● experimental data, — best fit). (inset) Plot of the magnetization vs magnetic field at 2 K (◆ experimental data, — best fit, - - - Brillouin curve for two spins of S = 1/2 and a g value of 2.1).

between the copper atoms separated by the oxo-bridging uranyl moiety [Cu1···Cu2 7.1359(16) Å] must be the most important one, but interactions between atoms belonging to two neighboring chains [Cu2···Cu2^{i} 7.766(2) Å, symmetry code i = 1 − x, 1 − y, 1 − z] via overlapping bipy groups cannot be neglected.[40] However, to estimate the maximum magnitude of the exchange we tried to fit the data with a simple dimer model where the exchange is represented by the spin Hamiltonian $\mathbf{H} = -2J\mathbf{S}_1\mathbf{S}_2$. Both the $\chi_M T$ versus T and the M versus H curves were fitted using the Magpack package[41] (Figure 13). The best fit corresponds to J = −0.4 cm^{-1} and g = 2.1 ($R = 8.3 \times 10^{-6}$).

CONCLUSIONS

Following our previous work on uranyl ion complexation by cyclohexane-based polycarboxylates (Kemp's triacid, 1,3-cyclohexanedicarboxylic, 1,3,5-cyclohexanetricarboxylic, and 1,2,3,4,5,6-cyclohexanehexacarboxylic acids), we have investigated the conformationally constrained 1,3-adamantanedicarboxylic acid, which had been the subject of only one report until now.[9] As in the cases of Kemp's triacid and 1,3,5-cyclohexanetricarboxylic acid, the experimental conditions for the synthesis of the complexes under solvo-hydrothermal

DOI: 10.1021/ic503004j
Inorg. Chem. 2015, 54, 2838−2850

conditions have been varied (organic cosolvent, additional 3d block metal cations, additional bipy coligand), which enabled isolation of eight different homo- or heterometallic complexes (one of them as two isomorphs), thus exemplifying once more the high sensitivity of these systems to modifications of the experimental setup. With respect to the triacids studied before, the reduced number of coordinating sites makes the present ligand a less favorable case for the synthesis of high-dimensionality polymers or even of discrete, closed species. However, it has been possible to isolate a 3D homometallic framework (complex **3**) based on a tris-chelated uranyl carboxylate motif, with dimethylammonium counterions generated in situ. Two cases are encountered when divalent 3d block additional cations (Co, Ni or Cu) are present. When the bipy coligand is added, it coordinates preferentially to the 3d metal cation and reduces consequently its ability to act as a bridging species; in this case, the $M(bipy)_x^{2+}$ moiety (x = 1−3) is either a decorating group attached to the uranyl-containing polymer (complexes **5**, **6**, and **9**) or a completely separated counterion (**7**), as was previously observed with Kemp's triacid.[7a] Only in the absence of bipy was it possible to generate a 3D uranyl−copper(II) framework in which both metal cations are part of the fabric of the polymer (**8**), this being one more example of the interest of using additional cations to increase the dimensionality in uranyl−organic assemblies. Emission spectra measured in the solid state display either well-resolved uranyl signals in the species devoid of 3d block metal ions (although very weak for **1**), or various degrees of quenching in the heterometallic complexes. Complex **7** is unusual in showing emission bands probably due to nickel(II) centers. In complexes **8** and **9**, the copper(II) cations are either magnetically isolated or display weak antiferromagnetic exchange, while zero-field splitting effects and possible antiferromagnetic intermolecular interactions are present in the nickel(II)-containing complex **6**.

■ ASSOCIATED CONTENT

Supporting Information

Tables of crystal data, atomic positions, and displacement parameters; anisotropic displacement parameters and bond lengths and bond angles in CIF format; additional views of the crystal structures of compounds **1**, **2**, **3**, and **6**; excitation spectra of compounds **1**, **4**, **5**, **6**, and **9**; magnetic properties of compounds **6** and **8**. This material is available free of charge via the Internet at http://pubs.acs.org.

■ AUTHOR INFORMATION

Corresponding Author

*E-mail: pierre.thuery@cea.fr.

Notes

The authors declare no competing financial interest.

■ REFERENCES

(1) For an overview of uranyl−organic assemblies, see: (a) Cahill, C. L.; de Lill, D. T.; Frisch, M. *CrystEngComm* **2007**, *9*, 15−26. (b) Cahill, C. L.; Borkowski, L. A. In *Structural Chemistry of Inorganic Actinide Compounds;* Krivovichev, S. V., Burns, P. C., Tananaev, I. G., Eds.; Elsevier: Amsterdam, Oxford, 2007; Ch. 11. (c) Wang, K. X.; Chen, J. S. *Acc. Chem. Res.* **2011**, *44*, 531−540. (d) Andrews, M. B.; Cahill, C. L. *Chem. Rev.* **2013**, *113*, 1121−1136. (e) Loiseau, T.; Mihalcea, I.; Henry, N.; Volkringer, C. *Coord. Chem. Rev.* **2014**, *266−267*, 69−109.

(2) (a) Kim, J. Y.; Norquist, A. J.; O'Hare, D. *Dalton Trans.* **2003**, 2813−2814. (b) Borkowski, L. A.; Cahill, C. L. *Acta Crystallogr., Sect. E: Struct. Rep. Online* **2004**, *60*, m198−m200. (c) Charushnikova, I. A.; Krot, N. N.; Polyakova, I. N.; Makarenkov, V. I. *Radiochemistry* **2005**, *47*, 241−246. (d) Yu, Z. T.; Liao, Z. L.; Jiang, Y. S.; Li, G. H.; Chen, J. S. *Chem.−Eur. J.* **2005**, *11*, 2642−2650. (e) Jiang, Y. S.; Yu, Z. T.; Liao, Z. L.; Li, G. H.; Chen, J. S. *Polyhedron* **2006**, *25*, 1359−1366. (f) Go, Y. B.; Wang, X.; Jacobson, A. J. *Inorg. Chem.* **2007**, *46*, 6594−6600. (g) Liao, Z. L.; Li, G. D.; Bi, M. H.; Chen, J. S. *Inorg. Chem.* **2008**, *47*, 4844−4853. (h) Liao, Z. L.; Li, G. D.; Wei, X.; Yu, Y.; Chen, J. S. *Eur. J. Inorg. Chem.* **2010**, 3780−3788. (i) Xia, Y.; Wang, K. X.; Chen, J. S. *Inorg. Chem. Commun.* **2010**, *13*, 1542−1547. (j) Mihalcea, I.; Henry, N.; Loiseau, T. *Cryst. Growth Des.* **2011**, *11*, 1940−1947. (k) Mihalcea, I.; Henry, N.; Clavier, N.; Dacheux, N.; Loiseau, T. *Inorg. Chem.* **2011**, *50*, 6243−6249. (l) Mihalcea, I.; Henry, N.; Volkringer, C.; Loiseau, T. *Cryst. Growth Des.* **2012**, *12*, 526−535. (m) Volkringer, C.; Henry, N.; Grandjean, S.; Loiseau, T. *J. Am. Chem. Soc.* **2012**, *134*, 1275−1283. (n) Mihalcea, I.; Henry, N.; Bousquet, T.; Volkringer, C.; Loiseau, T. *Cryst. Growth Des.* **2012**, *12*, 4641−4648. (o) Mihalcea, I.; Volkringer, C.; Henry, N.; Loiseau, T. *Inorg. Chem.* **2012**, *51*, 9610−9618. (p) Olchowka, J.; Falaise, C.; Volkringer, C.; Henry, N.; Loiseau, T. *Chem.−Eur. J.* **2013**, *19*, 2012−2022. (q) Olchowka, J.; Volkringer, C.; Henry, N.; Loiseau, T. *Eur. J. Inorg. Chem.* **2013**, 2109−2114. (r) Cantos, P. M.; Cahill, C. L. *Acta Crystallogr., Sect. E: Struct. Rep. Online* **2014**, *70*, m142−m143. (s) Mihalcea, I.; Henry, N.; Loiseau, T. *Eur. J. Inorg. Chem.* **2014**, 1322−1332.

(3) Thuéry, P. *CrystEngComm* **2009**, *11*, 232−234.

(4) Thuéry, P. *Cryst. Growth Des.* **2010**, *10*, 2061−2063.

(5) Thuéry, P.; Nierlich, M.; Baldwin, B. W.; Komatsuzaki, N.; Hirose, T. *J. Chem. Soc., Dalton Trans.* **1999**, 1047−1048.

(6) Thuéry, P.; Masci, B. *CrystEngComm* **2012**, *14*, 131−137.

(7) (a) Thuéry, P. *Cryst. Growth Des.* **2014**, *14*, 901−904. (b) Thuéry, P. *Cryst. Growth Des.* **2014**, *14*, 2665−2676.

(8) Thuéry, P.; Harrowfield, J. *Cryst. Growth Des.* **2014**, *14*, 4214−4225.

(9) Rusanova, J. A.; Rusanov, E. B.; Domasevitch, K. V. *Acta Crystallogr., Sect. C* **2010**, *66*, m207−m210.

(10) Sun, L. P.; Niu, S. Y.; Jin, J.; Yang, G. D.; Ye, L. *Eur. J. Inorg. Chem.* **2006**, 5130−5137.

(11) Hooft, R. W. W. *COLLECT;* Nonius BV: Delft, The Netherlands, 1998.

(12) Otwinowski, Z.; Minor, W. *Methods Enzymol.* **1997**, *276*, 307−326.

(13) (a) Sheldrick, G. M. *Acta Crystallogr., Sect. A* **2008**, *64*, 112−122. (b) Sheldrick, G. M. *Acta Crystallogr., Sect. C* **2015**, *71*, 3−8.

(14) Sheldrick, G. M. *Acta Crystallogr., Sect. A* **2015**, *71*, 3−8.

(15) Farrugia, L. J. *J. Appl. Crystallogr.* **1997**, *30*, 565.

(16) Momma, K.; Izumi, F. *J. Appl. Crystallogr.* **2008**, *41*, 653−658.

(17) (a) Blatov, V. A.; Shevchenko, A. P.; Serezhkin, V. N. *J. Appl. Crystallogr.* **2000**, *33*, 1193. (b) Blatov, V. A.; O'Keeffe, M.; Proserpio, D. M. *CrystEngComm* **2010**, *12*, 44−48.

(18) See, for example: (a) Chen, W.; Yuan, H. M.; Wang, J. Y.; Liu, Z. Y.; Xu, J. J.; Yang, M.; Chen, J. S. *J. Am. Chem. Soc.* **2003**, *125*, 9266−9267. (b) Yu, Z. T.; Liao, Z. L.; Jiang, Y. S.; Li, G. H.; Li, G. D.; Chen, J. S. *Chem. Commun.* **2004**, 1814−1815. (c) Luo, G. G.; Lin, L. R.; Huang, R. B.; Zheng, L. S. *Dalton Trans.* **2007**, 3868−3870. (d) Alsobrook, A. N.; Zhan, W.; Albrecht-Schmitt, T. E. *Inorg. Chem.* **2008**, *47*, 5177−5183. (e) Thuéry, P. *Inorg. Chem. Commun.* **2009**, *12*, 800−803. (f) Knope, K. E.; Cahill, C. L. *Eur. J. Inorg. Chem.* **2010**, 1177−1185. (g) Alsobrook, A. N.; Hauser, B. G.; Hupp, J. T.; Alekseev, E. V.; Depmeier, W.; Albrecht-Schmitt, T. E. *Chem. Commun.* **2010**, *46*, 9167−9169. (h) Alsobrook, A. N.; Hauser, B. G.; Hupp, J. T.; Alekseev, E. V.; Depmeier, W.; Albrecht-Schmitt, T. E. *Cryst. Growth Des.* **2011**, *11*, 1385−1393. (i) Thuéry, P. *CrystEngComm* **2013**, *15*, 6533−6545. (j) Thuéry, P.; Rivière, E. *Dalton Trans.* **2013**, *42*, 10551−10558. (k) Thuéry, P.; Harrowfield, J. *Cryst. Growth Des.* **2014**, *14*, 1314−1323. (l) Weng, Z.; Zhang, Z. H.; Olds, T.; Sterniczuk, M.; Burns, P. C. *Inorg. Chem.* **2014**, *53*, 7993−7998.

(19) See, for example: (a) Buckingham, D. A.; Harrowfield, J. M.; Sargeson, A. M. *J. Am. Chem. Soc.* **1974**, *96*, 1726−1729. (b) Paulet,

DOI: 10.1021/ic503004j
Inorg. Chem. 2015, 54, 2838−2850

C.; Loiseau, T.; Férey, G. *J. Mater. Chem.* **2000**, *10*, 1225−1229. (c) Chen, W.; Wang, J. Y.; Chen, C.; Yue, Q.; Yuan, H. M.; Chen, J. S.; Wang, S. N. *Inorg. Chem.* **2003**, *42*, 944−946. (d) Ganesan, S. V.; Lightfoot, P.; Natarajan, S. *Solid State Sci.* **2004**, *6*, 757−762. (e) Harrowfield, J. M.; Skelton, B. W.; White, A. H.; Wilner, F. R. *Inorg. Chim. Acta* **2004**, *357*, 2358−2364. (f) Zhao, J.; Li, J.; Ma, P.; Wang, J.; Niu, J. *Inorg. Chem. Commun.* **2009**, *12*, 450−453. (g) Bilyk, A.; Dunlop, J. W.; Fuller, R. O.; Hall, A. K.; Harrowfield, J. M.; Hosseini, M. W.; Koutsantonis, G. A.; Murray, I. W.; Skelton, B. W.; Stamps, R. L.; White, A. H. *Eur. J. Inorg. Chem.* **2010**, 2106−2126. (h) Thuéry, P. *Cryst. Growth Des.* **2011**, *11*, 2606−2620. (i) Thuéry, P. *Cryst. Growth Des.* **2011**, *11*, 3282−3294. (j) Thuéry, P. *Cryst. Growth Des.* **2012**, *12*, 499−507.

(20) Thuéry, P.; Masci, B.; Harrowfield, J. *Cryst. Growth Des.* **2013**, *13*, 3216−3224.

(21) Thuéry, P.; Harrowfield, J. *CrystEngComm* **2014**, *16*, 2996−3004.

(22) Knope, K. E.; Soderholm, L. *Chem. Rev.* **2013**, *113*, 944−994.

(23) Spek, A. L. *J. Appl. Crystallogr.* **2003**, *36*, 7−13.

(24) See, for example: (a) Van den Bossche, G.; Spirlet, M. R.; Rebizant, J.; Goffart, J. *Acta Crystallogr., Sect. C* **1987**, *43*, 837−839. (b) Turpeinen, U.; Hämäläinen, R.; Mutikainen, I.; Orama, O. *Acta Crystallogr., Sect. C* **1996**, *52*, 1169−1171. (c) Thuéry, P.; Nierlich, M.; Souley, B.; Asfari, Z.; Vicens, J. *J. Chem. Soc., Dalton Trans.* **1999**, 2589−2594. (d) Yu, Z. T.; Li, G. H.; Jiang, Y. S.; Xu, J. J.; Chen, J. S. *Dalton Trans.* **2003**, 4219−4220. (e) Crawford, M. J.; Mayer, P.; Nöth, H.; Suter, M. *Inorg. Chem.* **2004**, *43*, 6860−6862. (f) Harrowfield, J. M.; Skelton, B. W.; White, A. H. *C. R. Chim.* **2005**, *8*, 169−180. (g) Charushnikova, I. A.; Krot, N. N.; Polyakova, I. N.; Makarenkov, V. I. *Radiokhimiya* **2005**, *47*, 219−223. (h) Borkowski, L. A.; Cahill, C. L. *Cryst. Growth Des.* **2006**, *6*, 2248−2259. (i) Hennig, C.; Servaes, K.; Nockemann, P.; Van Hecke, K.; Van Meervelt, L.; Fluyt, L.; Wouters, J.; Görller-Walrand, C.; Van Deun, R. *Inorg. Chem.* **2008**, *47*, 2987−2993. (j) Thuéry, P. *Cryst. Growth Des.* **2008**, *8*, 4132−4143. (k) Rodríguez-Diéguez, A.; Mota, A. J.; Seco, J. M.; Palacios, M. A.; Romerosa, A.; Colacio, E. *Dalton Trans.* **2009**, 9578−9586. (l) Villiers, C.; Thuéry, P.; Ephritikhine, M. *Polyhedron* **2010**, *29*, 1593−1599.

(25) (a) Allen, F. H. *Acta Crystallogr., Sect. B* **2002**, *58*, 380−388. (b) Bruno, I. J.; Cole, J. C.; Edgington, P. R.; Kessler, M.; Macrae, C. F.; McCabe, P.; Pearson, J.; Taylor, R. *Acta Crystallogr., Sect. B* **2002**, *58*, 389−397.

(26) Thuéry, P. *CrystEngComm* **2009**, *11*, 1150−1156.

(27) (a) Siegel, S.; Hoekstra, H. R. *Acta Crystallogr., Sect. B* **1968**, *24*, 967−970. (b) Legros, J. P.; Jeannin, Y. *Acta Crystallogr., Sect. B* **1975**, *31*, 1133−1139. (c) Locock, A. J.; Burns, P. C. *Can. Mineral.* **2003**, *41*, 489−502. (d) Shvareva, T. Y.; Albrecht-Schmitt, T. E. *Inorg. Chem.* **2006**, *45*, 1900−1902. (e) Arnold, P. L.; Patel, D.; Blake, A. J.; Wilson, C.; Love, J. B. *J. Am. Chem. Soc.* **2006**, *128*, 9610−9611. (f) Arnold, P. L.; Patel, D.; Wilson, C.; Love, J. B. *Nature* **2008**, *451*, 315−317. (g) Thuéry, P.; Harrowfield, J. *Eur. J. Inorg. Chem.* **2014**, 4772−4778.

(28) (a) Burrows, H. D.; Kemp, T. J. *Chem. Soc. Rev.* **1974**, *3*, 139−165. (b) Denning, R. G. *Struct. Bonding (Berlin)* **1992**, *79*, 215−276. (c) Natrajan, L. *Coord. Chem. Rev.* **2012**, *256*, 1583−1603.

(29) Brachmann, A.; Geipel, G.; Bernhard, G.; Nitsche, H. *Radiochim. Acta* **2002**, *90*, 147−153.

(30) (a) Burrows, H. D.; Miguel, M.; da, G. *Adv. Colloid Interface Sci.* **2001**, *89*−*90*, 485−496. (b) Formosinho, S. J.; Burrows, H. D.; Miguel, M.; da, G.; Azenha, M. E. D. G.; Saraiva, I. M.; Ribeiro, A. C. D. N.; Khudyakov, I. G.; Gasanov, R. G.; Sarakha, M. *Photochem. Photobiol. Sci.* **2003**, *3*, 569−575. (c) Redmond, M. P.; Cornet, S. M.; Woodall, S. D.; Whittaker, D.; Collison, D.; Helliwell, M.; Natrajan, L. S. *Dalton Trans.* **2011**, *40*, 3914−3926.

(31) See, for example: (a) Alsobrook, A. N.; Zhan, W.; Albrecht-Schmitt, T. E. *Inorg. Chem.* **2008**, *47*, 5177−5183. (b) Heine, J.; Müller-Buschbaum, K. *Chem. Soc. Rev.* **2013**, *42*, 9232. (c) Kerr, A. T.; Cahill, C. L. *Cryst. Growth Des.* **2014**, *14*, 1914−1921.

(32) Ferguson, J.; Hawkins, C. J.; Kane-Maguire, N. A. P.; Lip, H. *Inorg. Chem.* **1969**, *8*, 771−779.

(33) Knope, K. E.; de Lill, D. T.; Rowland, C. E.; Cantos, P. M.; de Bettencourt-Dias, A.; Cahill, C. L. *Inorg. Chem.* **2012**, *51*, 201−206.

(34) Li, Y.; Su, J.; Mitchell, E.; Zhang, G. L.; Lu, J. *Sci. China Chem.* **2013**, *56*, 1671−1681.

(35) Burrows, H. D.; Formosinho, S. J.; Miguel, M.; da, G.; Pinto Coelho, F. *J. Chem. Soc., Faraday Trans. 1* **1975**, *71*, 163−171.

(36) Nelson, A. G. D.; Rak, Z.; Albrecht-Schmitt, T. E.; Ewing, R. C. *Inorg. Chem.* **2014**, *53*, 2787−2796.

(37) Kahn, O. *Molecular Magnetism;* VCH Publishers: New York, 1993.

(38) Lloret, F.; Julve, M.; Cano, J.; Ruiz-García, R.; Pardo, E. *Inorg. Chim. Acta* **2008**, *361*, 3432−3445.

(39) Boča, R. *Coord. Chem. Rev.* **2004**, *248*, 757−815.

(40) Sadhukhan, D.; Ray, A.; Pilet, G.; Rizzoli, C.; Rosair, G. M.; Gómez-García, C. J.; Signorella, S.; Bellú, S.; Mitra, S. *Inorg. Chem.* **2011**, *50*, 8326−8339.

(41) Borras-Almenar, J. J.; Clemente-Juan, J. M.; Coronado, E.; Tsukerblat, S. B. *J. Comput. Chem.* **2001**, *22*, 985−991.

NOTE ADDED AFTER ASAP PUBLICATION

This paper was published on the Web on February 24, 2015, with minor text errors. The corrected version was reposted on February 25, 2015.

DOI: 10.1021/ic503004j
Inorg. Chem. 2015, 54, 2838−2850